Journal of Physics: Conference Series **122** (2008) 012012 doi:10.1088/1742-6596/122/1/012012

Mechanical monolithic accelerometer for suspension inertial damping and low frequency seismic noise measurement

Fausto Acernese[1,2], Rosario De Rosa[2,3], Gerardo Giordano[2,3], Rocco Romano[1,2] and Fabrizio Barone[1,2]

[1] Department of Scienze Farmaceutiche, University of Salerno, Via Ponte Don Melillo, I-84084 Fisciano (SA), Italy
[2] INFN Sezione di Napoli, Complesso Universitario di Monte S.Angelo, Via Cintia, I-80126 Napoli, Italy
[3] Department of Scienze Fisiche, University of Napoli Federico II, Complesso Universitario di Monte S.Angelo, Via Cintia, I-80126 Napoli, Italy

E-mail: fabrizio.barone@na.infn.it

Abstract. This paper describes a mechanical monolithic tunable sensor prototype with elliptical hinges, shaped with electric-discharge-machining, that can be used both as seismometer and, in a force-feedback configuration, as accelerometer in the control of mechanical suspensions of interferometric gravitational waves detectors. The monolithic mechanical design and a laser optical readout make it a very compact instrument, very sensitive in the low-frequency seismic noise band and with a very good immunity to environmental noises. The theoretical sensitivity curves and the simulations show a very good agreement with the measurements. Very interesting scientific result its measured natural resonance frequency of $\approx 70\,mHz$ with a $Q \approx 140$ in air.

1. Introduction

The Folded Pendulum (hereafter FP), also known as *Watt-linkage*, is a system developed in 1962 [1], consisting of a simple pendulum and of an inverted pendulum connected together, as shown in Figure 1, recently been rediscovered for applications in gravitational wave research as ultra-low frequency mechanical isolator [2]. More recently, taking advantage of the progress in precision micro-machining, this architecture has been proposed for the implementation of single-axis monolithic accelerometers to be used as sensors for the control system of advanced mechanical attenuators [3]. In fact, a monolithic mechanical design has the great advantage of avoiding the shear effects at the contact surface among mechanical parts that can generate hysteresis and dissipation, resulting in a very compact sensor with a high Q-factor. The monolithic mechanical design guarantees also a very good sensor directivity: coupling factors of less than 10^{-4} among the different degrees of freedom have been obtained in monolithic structures [3]. A broadband single-axis monolithic Folded Pendulum of reasonable size with natural frequencies $\approx 700\,mHz$ has already been built [3]. Following this direction, we have developed an improved version of this monolithic seismic sensor, with good performances in terms of noise, sensitivity and frequency band. In the following sections we will describe the status of the monolithic FP sensor prototype and its mechanical and optical performances.

2. Monolithic Sensor Mechanical Model

An accurate description of the dynamics of a Folded Pendulum is given by the simplified lagrangian model developed by J.Liu et al. [2], shown in Figure 1. The FP is modeled as two vertical beams of lengths l_1 and l_2 and masses m_{a_1} and m_{a_2}, respectively. The central mass, which connects the beams, is modeled with two equivalent masses, m_{p_1} and m_{p_2}, located near the hinge points at distances l_{p_1} and l_{p_2} with respect to the pivot points of the pendulum arm and of the hinging point of the oscillating mass.

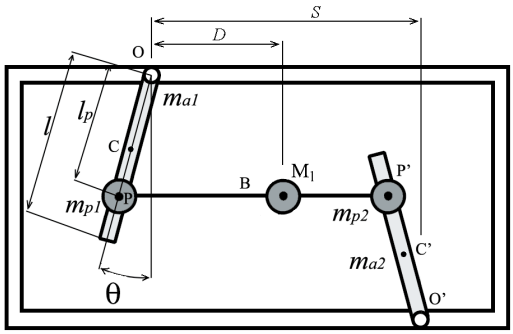

Figure 1. Folded Pendulum mechanical model

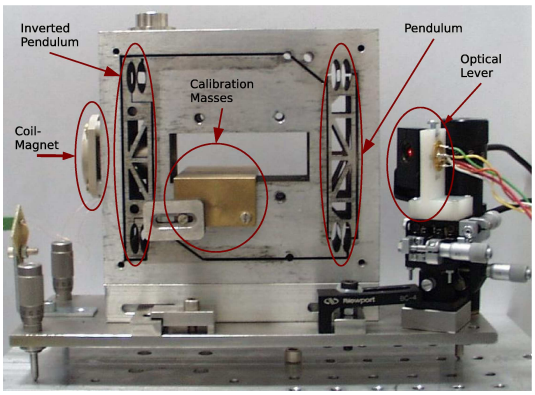

Figure 2. Picture of the monolithic FP Sensor.

Assuming that the center of mass of the pendula is in $l_i/2$ and using the approximation of small deflection angles, then potential energy of the FP is given by:

$$U = \frac{1}{2}\left(\frac{m_{a_1} g l_1}{2} - \frac{m_{a_2} g l_2}{2} + m_{p_1} g l_{p_1} - m_{p_2} g l_{p_2} + k\right)\theta^2 = \frac{1}{2}\mathcal{K}_{eq}\theta^2 \tag{1}$$

where θ is the angle of deflection, k is the cumulative angular stiffness of the joints and $\mathcal{K}_{eq}$ is the equivalent stiffness of the FP. The mechanical response of a FP to an external strain can be changed by modifying the shape of the potential energy: it is sufficient to change the values of the masses m_{p_1} and m_{p_2} by adding an external mass (tuning mass) M_l placed at a distance D from the pendulum suspension point, as shown in Figure 1. In fact, defining S as the distance between the FP hinges points, then the values of the masses m_{p_1} and m_{p_2} change according to the relations

$$m_{p_{1_{new}}} = m_{p_{1_{old}}} + M_l\left(1 - \frac{D}{S}\right) \quad \text{and} \quad m_{p_{2_{new}}} = m_{p_{2_{old}}} + M_l\left(\frac{D}{S}\right) \tag{2}$$

Therefore, the new values of the masses m_{p_1} and m_{p_2} change the value of the equivalent stiffness $\mathcal{K}_{eq}$, and, as consequence, the value of the potential energy and so the FP resonance frequency. Hence, as a conclusion, the FP resonance frequency can be easily modified by changing the value, M_l, and the position, D, of a tuning mass.

Defining the coordinates of the pendulum frame (fixed to the ground), x_s, and of the FP central mass, x_p, (see Figure 1), then the mass displacement transfer function with respect to the ground displacement is

$$\frac{x_p - x_s}{x_s} = \frac{(1 - A_c)\omega^2}{\omega_0^2 - \omega^2} \tag{3}$$

where

$$\omega_0^2 = \frac{g}{l_p} \cdot \frac{(m_{a_1} - m_{a_2})\frac{l}{2l_p} + (m_{p_1} - m_{p_2}) + \frac{k}{g l_p}}{(m_{a_1} + m_{a_2})\frac{l^2}{3l_p^2} + (m_{p_1} + m_{p_2})} \tag{4}$$

is the FP resonant angular frequency and A_c is the parameter related to the centre of percussion effects [3].

3. The monolithic folded pendulum prototype

The FP mechanical monolithic sensor prototype has been implemented in Aluminum (Alloy 7075-T6), shaped with electric discharge machining (EDM) [4], [5]. Aluminum is a very good material for our purpose due to its good thermal conductivity, immunity to electromagnetic fields, good elastic properties and low internal friction characteristics, with the further advantage that it is not expensive and the EDM is relatively easy. The monolithic FP sensor prototype is shown in Figure 2. The monolithic FP sensor has been obtained by machining a $134\times134\times40\,mm$ bulk of metal. The four torsional flexures, connecting the pendulum arms to the central mass and to the frame, are elliptical notch hinges $100\,\mu m$ thick with ellipticity ration of $\epsilon = 16/5$. The pendula arms ($81.5\,mm$ length and spaced by $102\,mm$) are designed to minimize the mass and the moment of inertia without reducing rigidity and symmetry. The gap between the central mass and the external frame is large $1\,mm$ to reduce the effects of friction with air. In fact, the original FP sensor has a very high Q in vacuum ($Q \approx 3000$), very close to the theoretical value for Aluminum, but this decreases down to a value of $Q \approx 3$ in air. The gap enlargement has produced a large increase of the Q in air ($Q \approx 140$). Moreover, the values of the masses of the pendulum arm, of the inverted pendulum arm and of the central mass are $m_{a_1} \approx 40\,g$, $m_{a_2} \approx 50\,g$ and $(m_{p_1} + m_{p_2}) \approx 600\,g$ respectively. A mass of $336\,g$ is positioned in the opening of the central mass for the FP resonance frequency tuning. Two more tuning masses of $40\,g$ each are used instead for a more accurate calibration. The FP readout is instead based on laser optics techniques (optical lever and interferometry). Finally, the sensor is positioned on a platform for its levelling.

3.1. Elliptical hinges

The most critical part of the FP are the eight flex joints supporting the test mass, whose angular stiffness can be modeled using the Tseytlin formula [6], that is

$$k = \frac{Eat^2}{16[1 + \sqrt{1 + 0.215(2\epsilon R/t)}} \tag{5}$$

where a is the width of the joint, t is the thickness at the center, R is the radius of curvature, E is the Young's modulus of the material and ϵ is the hinge ellipticity; the first series of monolithic FP sensors is characterized by circular notch hinges ($\epsilon = 1$), actual accelerometers have $\epsilon = 3.2$.

Analyzing with finite elements method the characteristic of elliptical hinge, using the COMSOL© simulation program, we see (Figure 3) that the natural frequency of an hinge, with a tensile stress similar to a typical stress of one hinge of the accelerometer, decrease to the increasing of the ellipticity of the hinge, as it is also clear from Equation 5. In particular we note that the stress is below the elastic limit of $550\,MPa$ of the material when the hinge has the maximum deformation (corresponding to an extreme position of the test mass), that is a guarantee of robustness and long-term durability of the mechanics. This trend have also a recoil on the behavior of the frequency of an ideal hinge (the analysis is made only on an hinge without oscillating mass), demonstrating that the frequency contribution is minor with high ellipticity.

3.2. Optical Readout

The readout system of the sensor is based on laser optics. This solution gives a very high readout sensitivity together with very low coupling effects with environmental noises. The optical readout system, shown in Figure 4, is basically a combination of an optical lever and a homodyne Michelson interferometer. This redundancy was introduced in order to compare the

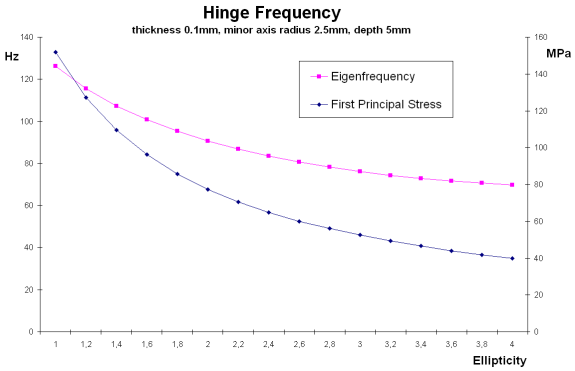

Figure 3. Eigenfrequencies and the first principal stress of the hinge as function of the hinge ellipticity, ϵ.

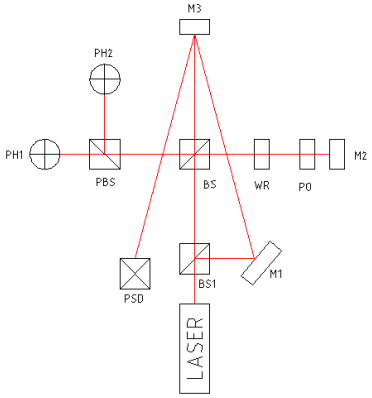

Figure 4. Optical scheme of the implemented readout system.

sensitivities of the two readout systems with respect to the theoretical ones and to test a two-step control strategy. The two steps of the control strategy are shortly described in the following. At the startup, the optical lever provides the error signal for the FP in order to reduce, within an interferometric fringe, the movement of the mirror M3, attached to the inertial mass (step one). Then, the Michelson interferometer provides a more accurate error signal, allowing the locking of the test mass position with respect to the frame (step two).

The optical readout works in a very simple way. The stabilised laser beam ($\lambda = 632.8\,nm$, $P = 3mW$) is divided into two beams by the cubic beam splitter BS_1. The first beam, reflected by the mirror M_1, and the $2D$ Position Sensor Detector (PSD S2044 by Hamamatsu©) are used to implement an optical lever to measure the position of mirror M_3, that is attached to the lateral side of the sensor test mass. The signals, coming from PSD, are combined and amplified using an ad hoc developed electronic board. Therefore, the optical lever provides a signal, that after some elaboration, is proportional to the relative motion of the test mass with respect to the sensor frame. The second beam is used for the implementation of a polarimetric homodyne Michelson interferometer [7], consisting of the beam splitter BS, the $\lambda/4$ retarder (WR), the polarizing plate $P0$, the reference mirror M_2 and mirror M_3. The interference beam is split using a polarised beam splitter (PBS). Then the polarised beam is read by the photodiodes PH_1 and PH_2 always differing each other of 1/4 of a fringe (or $\pi/2$). Finally, the mirror displacement is reconstructed with a quadrature correction algorithm and a phase-unwrapping technique [8].

4. Experimental Results

The first series of tests were related to demonstrate the possibility of mechanically tuning its natural frequency at values better that $100\,mHz$, a frequency low enough for application in mechanical suspensions of interferometric detectors. For these tests we have used both the tuning mass of $336\,g$ and the fine tuning masses of $40\,g$ each placed in the central opening, as shown in Figure 2. The tuning masses have been moved in small steps, of less than $1\,mm$. The resonant frequency and the quality coefficient were evaluated measuring the amplitude and the time distance between two, or more peaks of the step response of FP in the time domain.

We have made several sets of measurement in order to evaluate the stability of the measurement procedure. In Figure 5 the measured frequency versus the tuning mass position are shown for different sets of measurements. The data have been interpolated using Equation 3 with adaptive parameters $(m_{p_1} + m_{p_2})$ and k. Figure 5 shows the very good agreement between the experimental data and the 3σ error bars of the theoretical model. The interpolated parameters with an error bar with a level of significance $\alpha = 0.05$ are in good agreement with

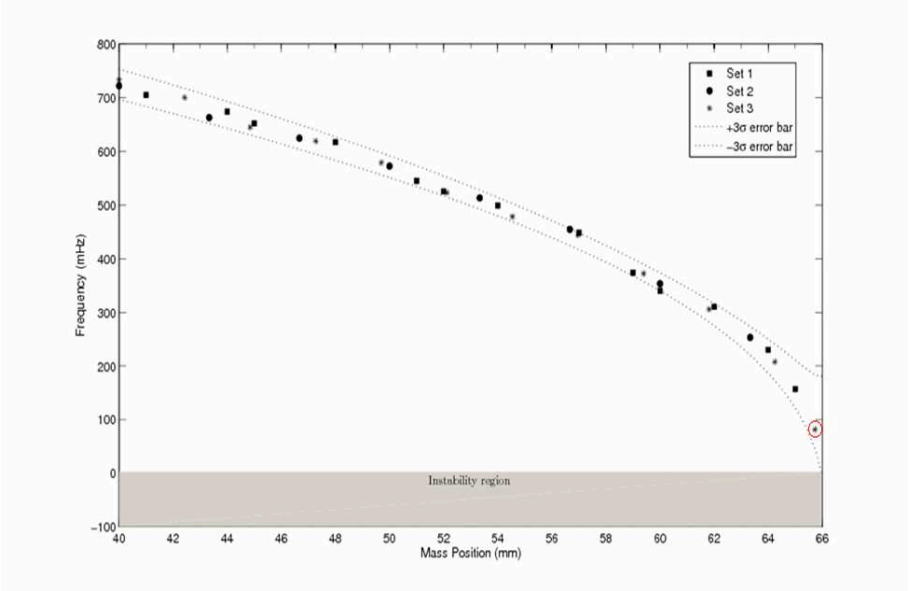

Figure 5. Measured natural resonance frequencies of the monolithic folded pendulum sensor prototype. The best measured frequency, $f_r = 70\,mHz$, is circled.

the experimental ones, such as the distributed masses and the angular stiffness interpolated are in good agreement with the measured ones in this case, too. The lowest natural frequency measured is about $70\,mHz$, that is a very good result for a monolithic FP sensor with these dimensions, if one takes into account also the measured Q of the FP that is $Q \approx 140$. Note that the position of the calibration mass has been fixed with an accuracy of about $\pm 1\,mm$ in this experimental setup. Considering Figure 5, we note that to further decrease the natural frequency without reaching the FP instability, it is necessary to improve the calibration procedure, refining the tuning mass positioning system.

The second series of tests has been aimed to evaluate the sensitivity curve of the monolithic FP sensors using the two optical readout systems, the optical lever and the Michelson interferometer. Actually up to now we have performed only measurements with the optical lever readout, being the test phase on the Michelson interferometer readout still at the beginning. The double readout system has been developed for signal validation, as a backup readout system in case of failures and for control strategies testing. We remind here that all the tests were performed in air, with no thermal stabilization and with the FP sensor clamped. The results of these tests are shown in Figure 6. In this figure the measured FP sensing noise is shown together with the theoretical sensing noise. Moreover, the best theoretical sensitivity curves for the monolithic FP sensor at $T = 300\,K$ with laser optical lever and laser interferometric readouts are shown. For completeness and for understanding the monolithic FP sensor real sensitivity limits, the theoretical thermal noise, the Peterson New Low Noise Model (NLNM) [9] and the Newtonian noise [10]are shown. The tests in closed loop configuration (force-feedback) have just started. In this configuration the sensor behaves like an accelerometer. Preliminary results seems to be quite good.

5. Conclusions

We have described a mechanical monolithic tunable sensor protoype with elliptical hinges, shaped with EDM, that can be used both as seismometer and, in a force-feedback configuration, as accelerometer in the mechanical suspensions control of gravitational waves interferometric

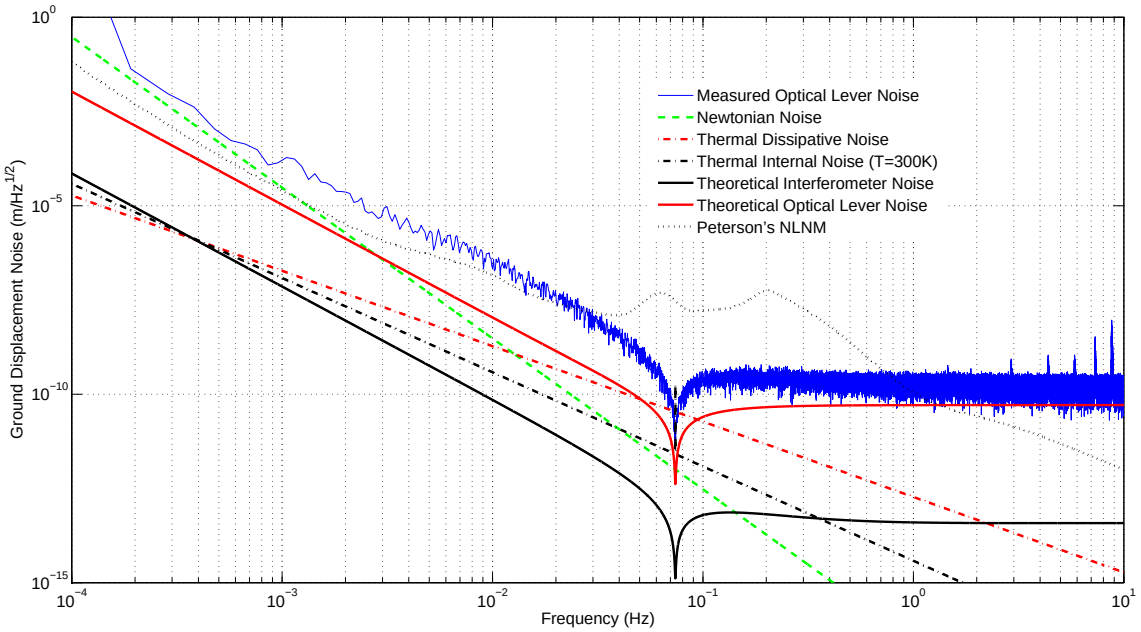

Figure 6. Theoretical and experimental noise curves of the monolithic FP sensor prototype with optical lever and laser interferometric readouts.

detectors. The monolithic mechanical design and the laser optical redout make it a very compact sensor, very sensitive in the low-frequency seismic noise band and with a good immunity to environmental noises. The theoretical sensitivity curves and the simulations show a good agreement with the measurements. Very interesting scientific result is the measured natural resonance frequency of $\approx 70\,mHz$ with a $Q \approx 140$ in air. Further tests are planned to evaluate its performances as accelerometer, although preliminary results seem to be very positive.

Acknowledgments

We acknowledge Mr. Carlo Galli (Galli & Morelli Factory) for the useful suggestions and for the technical support in the development and implementation of FP prototype mechanics.

References

[1] Fergusson E S 1962, *US Nat. Museum Bull.* **228** 185
[2] Liu J, Ju L and Blair D G 1997 *Phys. Lett. A* **228** 243
[3] Bertolini A et al. 2006 *Nucl. Instr. and Meth.* **556** 616
[4] Acernese F, De Rosa R, Garufi F, Romano R, Barone F 2006 Proc. of SPIE *Remote Sensing for Environmental Monitoring, GIS Applications, and Geology VI*, Stockholm, Sweden, September 11-16, **6366** 63660I-1
[5] Acernese F, De Rosa R, Giordano G, Romano R, Barone F 2007 Proc. of SPIE *SPIE Sensors and Smart Structures and Technologies for Civil, Mechanical and Aerospaced Systems*, San Diego, California (USA), March 18-22, **6529** 65292B-1
[6] Tseytlin M Y 2002 *Rev. Sci. Instrument* **73** 3363
[7] Wu C M et al. 1996 *Metrologia* **33** 533
[8] István D 2005 *Measurement* **37** 95
[9] Berger J and Davis P 2005 *2005 IRIS 5-Year Proposal* 38
[10] Punturo M 2004, VIR-NOT-PER-1390-51, *Virgo Internal Report*